On-Chip Indoor-Outdoor Cold-Startup Circuit for Miniature Photovoltaic Cells

Vasiliki Gogolou, Konstantinos Kozalakis, Stylianos Siskos
Electronics Lab, Physics Dept., Aristotle Univ. of Thessaloniki, Thessaloniki, Greece
vgogolou@physics.auth.gr, kkozalak@physics.auth.gr, siskos@physics.auth.gr

***Abstract*—This work presents experimental results from an integrated low-power, low-area Dickson charge pump circuit, using 7.5 mm^2 miniature photovoltaic cells, for cold-start operation. The proposed cold-start topology presents successful operation, both for indoor and outdoor lighting conditions, for input voltages as low as 440 mV. The cold-start circuit is implemented and fabricated in a 0.18 um CMOS process. The chip active area, occupied by the designed cold-start block, is 0.224 mm^2. The area-efficient and low-power design of the presented cold-start circuit makes it ideal for micro-energy harvesting applications.**

Keywords—Charge pump, Dickson, cold start, integrated, low-power, photovoltaic cell, indoor, outdoor, energy harvesting

I. INTRODUCTION

In today's world, the energy harvesting concept is widely used for the power supply of a great number of applications in various fields. Wireless sensor networks, portable and wearable devices, biomedical implants are a few application examples which demand constant, reliable power supply and small-sized solutions in order to be efficient [1]. In most cases, the preferable storage element is the capacitor due to its smaller size and longer lifetime, compared to the battery. For this reason, the utilization of micro-generators which exploit renewable energy sources such as light, heat and micro-vibrations are an attractive solution for this kind of applications [2].

Among the available ambient energy sources alternatives, light energy harvesting via photovoltaic cells is the most popular method. A typical light energy harvesting system depends on a primary conversion circuit (i.e., an inductive boost DC-DC converter) to extract the available energy of the connected photovoltaic cell (Figure 1). However, the proper operation of such a circuit depends on a control block which consists of circuits such as clocks, driver buffers, PWM generators, which demand a certain voltage supply level, many times higher than the voltage offered from the photovoltaic cell (~400-600 mV). Therefore, the system cannot kick-start by itself after energy starvation periods. As light energy harvesting cannot be considered continuous, this phenomenon poses a serious problem regarding the uninterrupted operation of the energy harvesting system and the connected loads (e.g., sensor modules, transmitters, microcontrollers etc.).

To this end, cold-start circuits are implemented in order to provide self-startup operation and reliability to the energy harvesting systems. Most published works propose solutions which can be classified in two different categories. The first one is mechanically assisted topologies utilizing MEM switches or external bulky transformers [3-5]. The second one is based on switched-capacitor voltage converter topologies, i.e., charge pump circuits. This last approach proves to be the most efficient for size-restrained applications as it can be fully integrated on-chip, eliminating bulky external components such as inductors or large capacitors. Many works have been proposed in literature exploiting various charge pump topologies such as Dickson, cross-coupled switched capacitor converters and hybrid implementations which combine different techniques [6]. Most of these solutions use quite large photovoltaic cells (>1cm^2), or photovoltaic arrays in order to provide cold-start operation in indoor low-lighting conditions or provide integrated circuit solutions which cover large active die area [7-9].

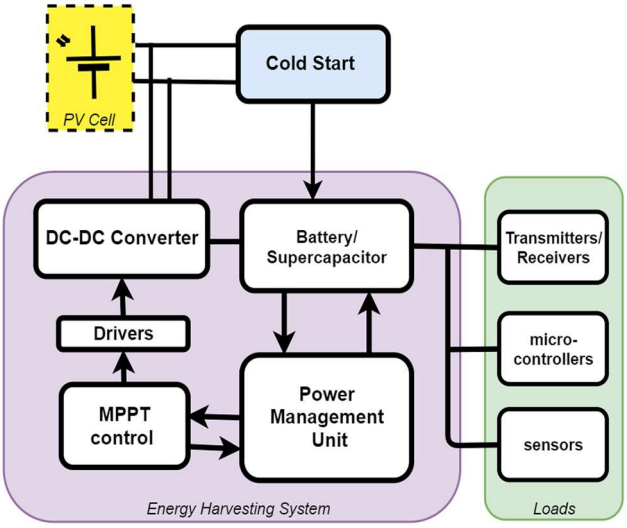

Fig.1 Block diagramm of a light energy harvesting system.

In this work, an integrated low-power charge pump is presented, suitable for cold-start operation both in indoor and outdoor lighting conditions for micro-energy harvesting applications, based on the Dickson topology [10]. The circuit's design aims to efficient operation when connected to miniature photovoltaic cells. The Dickson topology is chosen, for its simplicity and low-complexity characteristics. The proposed circuit utilizes diode-connected 3.3V native NMOS transistors for each stage, in order to exploit the ultra-low threshold that these devices present. The control block utilizes an ultra-low power ring oscillator and a non-overlapping clock generator which produces the driving signals for the pumping capacitors.

The rest of the paper is organized as follows: Section II describes the design challenges regarding specifications trade-offs and technology related restrictions of a charge pump circuit. Section III presents the proposed cold-start circuit topology and simulation results, and Section IV provides the experimental results of the chip measurement, exploiting photovoltaic cells under various lighting conditions. Finally, Section V concludes this paper.

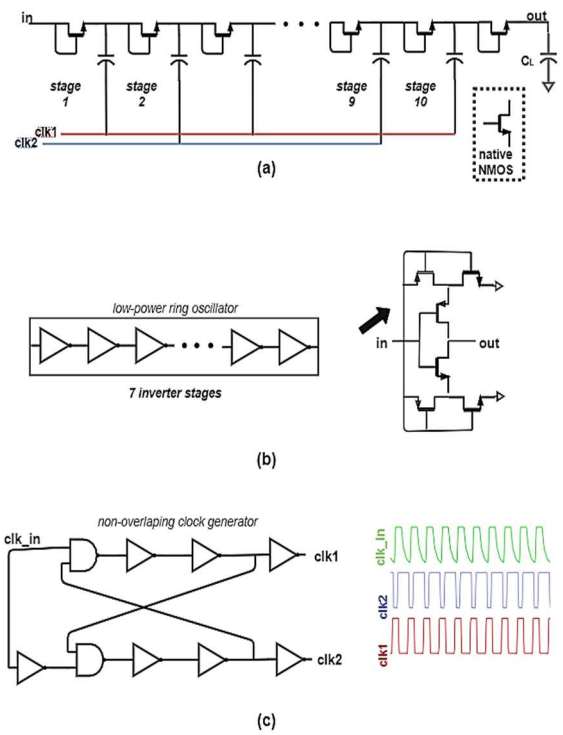

Fig. 2. Cold-start topology. (a) Dickson charge pump circuit with diode-connected native NMOS transistors. (b) low-voltage low-power ring oscillator and stacked inverter circuit. (c) non-overlapping clock generator producing two-phase pulses.

II. Design Considerations

While designing a charge pump circuit, design parameters such as number of stages, desired output voltage, control block power consumption, active die area and charge dissipation during rise time must be taken under consideration.

The charge pump's equivalent resistance is [11]:

$$R_{eq} = \frac{N}{C \cdot f} \qquad (1)$$

where N is the number of stages, C is the value of the pumping capacitance of each stage and f is the switching frequency of the charge pump. Thus, considering high input power levels, a small number of stages and large pumping capacitances with high switching frequency is in need, for minimization of the equivalent resistance and maximum output current delivery. However, the charge consumption, Q_T, at rise time described in Equation 2 should be considered [11]. Q_L factor represents the charge delivered to the output, Q_{pump} is the charge drawn by the pumping capacitances of the charge pump and finally, Q_{par} is the charge portion consumed by the parasitic capacitances.

$$Q_T = Q_L + Q_{pump} + Q_{par} \qquad (2)$$

Equation 3 describes in more detail the relation of the charge pump design parameters with the charge consumption [11].

$$Q_T = (N+1)(C_{eq} + C_L)\left[(V_o(t_r) - V_o(0)\right] + a \cdot C_T \cdot V_{DD} \cdot \frac{t_r}{T} \qquad (3)$$

C_{eq} is the equivalent capacitance of the charge pump, C_L the output capacitor, t_r the rise time of the output voltage, C_T the sum of the pumping capacitances, V_{DD} the input voltage and T the clock period. The factor a depends on the used process and is associated with the charge losses on the parasitic capacitances created at the terminals of the pumping capacitances. For lighting conditions that provide low power to the cold-start input (i.e., indoor light) the charge portion wasted on the parasitic capacitances increases and therefore additional stages, smaller pumping capacitances and lower switching frequency are need. Hence, depending on the lighting conditions, i.e., the available input power levels, the design of the cold-start circuit presents some trade-offs [12].

III. Cold Start Topology

The cold-start circuit presented in this work, is designed according to the considerations described above. The topology is optimized in order to provide cold-start operation in low lighting conditions. Figure 2 depicts the schematic of the cold-start circuit. The Dickson charge pump consists of ten stages to ensure the desirable output voltage in case of load connection or output capacitor leaks.

The conventional Dickson charge pump circuit structure presents a low pumping capacity due to the large threshold voltage (~500-700mV) of the diode-connected transistors used in each stage. In modern CMOS technologies, devices such as low-threshold transistors are available, or zero-threshold native devices. The technology used in this work provides native 3.3 V NMOS devices with a voltage threshold rated at ~180 mV. For the pumping capacitances needed for each stage, metal-insulator-metal (MIM) capacitors are used due to the large capacitive density and low leakage currents that they present, compared with the alternative options, available in this technology. Each stage utilizes a 16-pF pumping capacitance.

The control circuit of the proposed topology utilizes a clock implemented with a ring oscillator circuit based on [13]. Since cold-start circuits normally suffer from poor power conversion efficiency, a non-overlapping clock generator is used which provides two-phase clock input pulses for the pumping capacitances with a dead time, avoiding this way simultaneous operation of n and n+1 stage, which would result significant power loss [14]. For the proper driving of the pumping capacitances, tapped drivers are connected to the terminal of the capacitances.

The minimum desired output voltage is set to 2 V. This specific threshold is selected since it is considered a safe voltage supply for the control circuits of the primary energy harvesting system to startup. Figure 3a depicts the simulated output transients, for input voltages from 440 mV to 1 V. 440 mV is the minimum input voltage that provides safe operation (passes process-voltage-temperature corner analysis) according to the simulation results. The output capacitor is 1 nF and a resistor of 10 MΩ is connected, to emulate the oscilloscope's probe load. As depicted, the circuit provides voltage outputs over 2 V. In the final system, a control circuit will monitor the output voltage, to activate the primary system at the desired threshold and to also secure operation within the maximum voltage ratings (3.6 V maximum). The ten-stage configuration enables charging speedup, as well as reaching the desired output threshold, in case of higher leakages.

For the 440 mV to 1 V input range, the ring oscillator provides a switching frequency of 190 kHz to 830 kHz (Fig 3b). The control unit's power consumption is calculated at 5.6 uA at 440 mV.

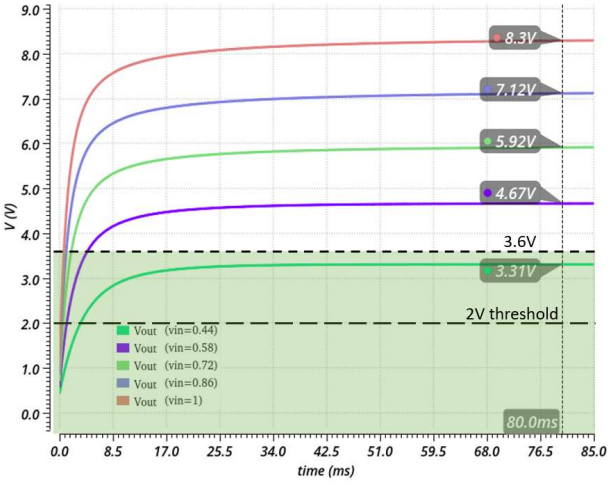

(a)

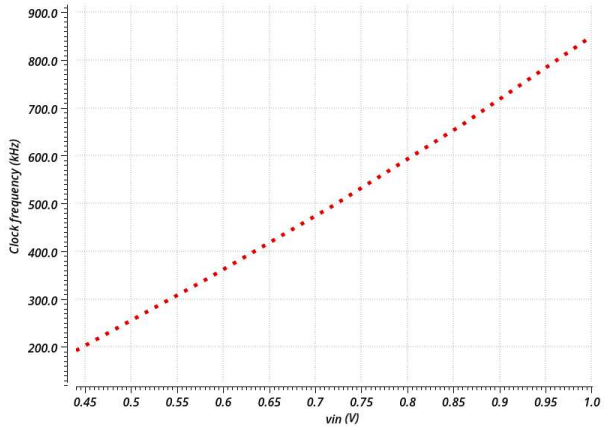

(b)

Fig. 3. a) Simulated transient response of the cold-start circuit and b) clock frequency, versus input voltage values.

IV. Experimental Results

The cold-start circuit is implemented and fabricated on-chip in a 0.18 um CMOS process. Figure 4 present the physical design and the die photo, under microscope view. The active silicon area of the proposed cold-start circuit is 0.224 mm^2. The MIM pumping capacitors cover 0.20 mm^2, while the control circuits only 0.0229 mm^2.

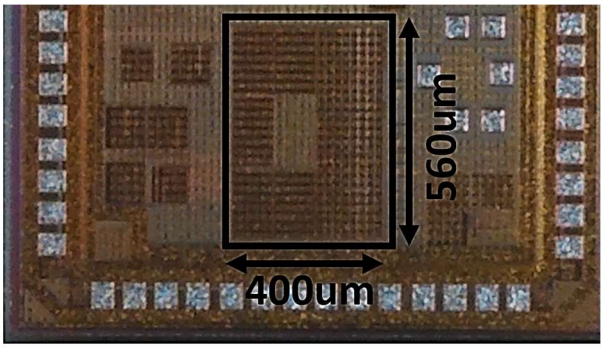

Fig. 4. Physical design and photo of the fabricated die.

To test the fabricated cold-start an external SMD capacitor of 10 uF value is connected at the output of the circuit, to store the harvested energy. It should be noted that depending on the system under consideration and the purpose of the cold-start (i.e., startup of the control circuits of the overall energy harvesting system or burst mode of the primary DC-DC converter to kick-start the system) the output capacitor should be selected accordingly.

To test the cold-start topology under realistic energy availability conditions, of-the-shelf photovoltaic cells are used. Specifically, the VISHAY miniaturized BPW34 photovoltaic cells [15] (Figure 5). These devices are selected since their specifications are suitable for area-restrained portable applications. The BPW34 photovoltaic cells present a radiant-sensitive area of 7.5 mm^2, with a rated open circuit voltage of 350 mV (at 900nm, 1mW/cm^2 light source), and short circuit current 47 uA.

The measurement setup is depicted in Figure 6. Six photovoltaic cells are available for connection in series and/or parallel configurations. A custom-made tunable light source is used to radiate the photovoltaic cells and a UNI-T UT383 lux meter is also used in order to provide detailed monitoring of the light intensity variations during the measurements. To measure the output voltage levels, a Siglent SDS1102CML+ oscilloscope is used. The cold-start circuit is tested under different illuminations, emulating different lighting conditions for indoor or outdoor energy harvesting application scenarios. To protect the chip from overvoltage, a 3 V low-leakage Zener diode is connected at the circuit's output.

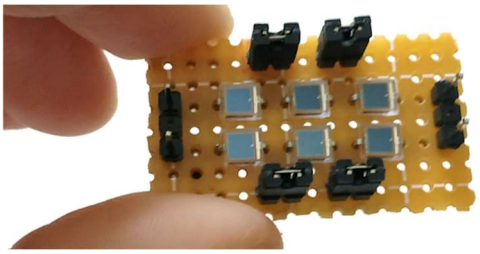

Fig. 5. BPW34 miniature photovoltaic cells used in series-parallel configuration.

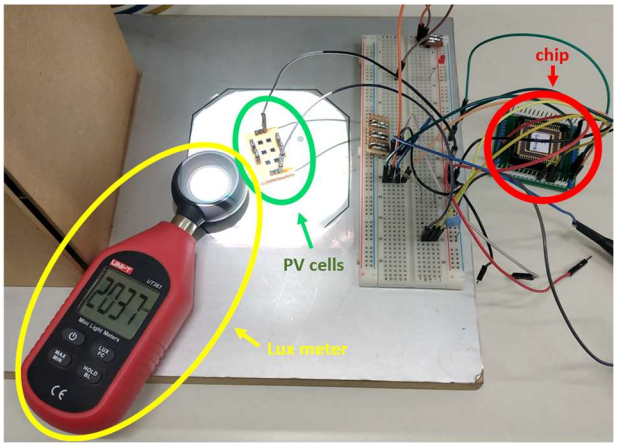

Fig. 6. Measurements setup of the fabricated cold start circuit under varying lighting conditions.

The tested light intensity range is between 460 lux (indoor office lighting) and 90.000 lux (non-direct sunlight). Table I presents the output rise time for the cold-start circuit to reach the voltage level of 2 V, for six different photovoltaic cells configurations. As presented, the cold-start circuit can

TABLE I. MEASURED RISE TIME VALUES FOR SERIES-PARALLEL CONFIGURATIONS OF PHOTOVOLTAIC CELLS.

	Photovoltaic Cells Configurations*						
Lux	**1**	**1+1**	**1+1+1**	**1+1+1+1**	**1//1**	**(1+1)//(1+1)**	**(1+1+1)//(1+1+1)**
460	-	-	-	-	-	125s	115s
900	-	175s	170s	305s	-	33s	30s
20000	175s	6.3s	3.1s	2.5s	165s	6.2s	3s
90000	34s	4.3s	1.925s	1.25s	34.75s	4.2s	1.8s

*+ series connection, // parallel configuration

properly work for both indoor and outdoor lighting conditions and start-up the connected energy harvesting system. For indoor lighting conditions, at least two photovoltaic cells are needed, due to the minimum input voltage restriction. However, in outdoor conditions the voltage provided by one single miniature cell is sufficient and the cold-start can effectively start-up the connected system in a few seconds. Figure 7 depicts the transient response of the cold-start under 2037 lux and three cells connected in series.

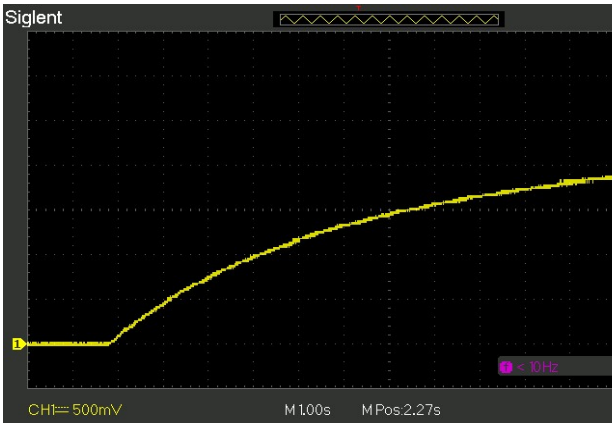

Fig. 7. Transient response of the cold-start circuit. Output voltage under 2037 lux for three cells connected in series.

V. CONCLUSIONS

In this work, a cold-start circuit based on a Dickson charge pump is presented, suitable for miniaturized photovoltaic cells both for indoor and outdoor lighting conditions. The circuit is fully integrated on-chip in a 0.18 um CMOS process, utilizing 3.3 V native NMOS devices for the successful decrease of the minimum input voltage. The proposed circuit is active area efficient, occupying only 0.224 mm^2 and is able to kick start the operation of a primary DC-DC boost converter of an energy harvesting system from input voltage as low as 440 mV. The experimental results utilizing miniature of-the-self photovoltaic cells under various lighting conditions validate the successful operation of the cold-start topology.

Future work will be focused on the integration of the cold-start circuit in a real light energy harvesting system and to be tested in indoor and outdoor conditions, in order to verify the operation of the overall system under a real wireless sensor application.

ACKNOWLEDGMENT

This research has been co - financed by the European Regional Development Fund of the European Union and Competitiveness, Entrepreneurship, and Innovation, under the call RESEARCH – CREATE – INNOVATE (project code: T1EDK-00360).

REFERENCES

[1] C. Xu, Y. Song, M. Han, et al. “Portable and wearable self-powered systems based on emerging energy harvesting technology”. *Microsyst Nanoeng* 7, 25 (2021).

[2] L. Colalongo, D. I. Leu, A. Richelli and Z. Kovacs, "Ultra-Low Voltage Push-Pull Converter for Micro Energy Harvesting," *in IEEE Transactions on Circuits and Systems II: Express Briefs*, vol. 67, no. 12, pp. 3172-3176, Dec. 2020

[3] Y. K. Ramadass and A. P. Chandrakasan, “A battery-less thermoelectric energy harvesting interface circuit with 35 mV startup voltage,” *IEEE J. Solid-State Circuits*, vol. 46, no. 1, pp. 333–341, Jan. 2011.

[4] J.-P. Im, S.-W. Wang, S.-T. Ryu, and G.-H. Cho, “A 40 mV transformerreuse self-startup boost converter with MPPT control for thermoelectric energy harvesting,” *IEEE J. Solid-State Circuits*, vol. 47, no. 12.

[5] A. Romani, A. Camarda, A. Baldazzi and M. Tartagni, "A micropower energy harvesting circuit with piezoelectric transformer-based ultra-low voltage start-up," *2015 IEEE/ACM International Symposium on Low Power Electronics and Design (ISLPED)*, 2015, pp. 279-284.

[6] L. F. Rahman, M. Marufuzzaman, L. Alam, and M. B. Mokhtar, “Design Topologies of a CMOS Charge Pump Circuit for Low Power Applications,” *Electronics*, vol. 10, no. 6, p. 676, Mar. 2021.

[7] D. K. W. Li, M. Ashourloo, M. Rose, H. J. Bergveld and O. Trescases, "Integrated switched-capacitor-based cold-start circuit for DC-DC energy harvesters with wide input/output voltage range and low inductance in 40-nm CMOS," *2018 IEEE Applied Power Electronics Conference and Exposition (APEC)*, 2018, pp. 2104-2109.

[8] X. Liu and E. Sanchez-Sinencio, “A highly efficient ultralow photovoltaic power harvesting system with MPPT for Internet of Things smart nodes,” *IEEE Trans. Very Large Scale Integr. (VLSI)* Syst., vol. 23, no. 12, pp. 3065–3075, Dec. 2015.

[9] F. Fraternali, B. Balaji, Y. Agarwal, L. Benini, and R. Gupta, “Pible: Battery-free mote for perpetual indoor ble applications: Demo abstract,” in Proc. 5th Conf. Syst. Built Environ. (BuildSys), 2018, pp. 184–185.

[10] J. F. Dickson, “On-chip high-voltage generation in NMOS integrated circuits using an improved voltage multiplier technique,” IEEE Journal of Solid-State Circuits, vol. 11, no. 3, pp. 374–378, Jun 1976.

[11] G. Palumbo and D. Pappalardo, “Charge pump circuits: An overview on design strategies and topologies,” *IEEE Circuits Syst. Mag.*, vol. 10, no. 1, pp. 31–45, First Quarter 2010.

[12] D. Cabello, E. Ferro, O. Pereira-Rial, B. Martinez-Vazquez, V. M. Brea, J. M. Carrillo, and P. Lopez, ‘‘On-chip solar energy harvester and PMU with cold start-up and regulated output voltage for biomedical applications,’’ *IEEE Trans. Circuits Syst. I, Reg. Papers,* vol. 67, no. 4, pp. 1103–1114, Apr. 2020.

[13] S. Bose and M. L. Johnston, “A stacked-inverter ring oscillator for 50 mV fully-integrated cold-start of energy harvesters,” in Proc. IEEE Int. Symp. Circuits Syst. (ISCAS), May 2018, pp. 1–5.

[14] H. Milton, F. Catthoor, “A Robust Two-Phase On-Chip Clock Generator”, *Solid-State Circuits Conference*, IEEE, vol. 1, pp. 19-21, 2003.

[15] Available online : https://www.vishay.com/docs/81521/bpw34.pdf